Quaternary Research 75 (2011) 80–90

Contents lists available at ScienceDirect

Quaternary Research

journal homepage: www.elsevier.com/locate/yqres

Geomorphic and climatic change over the past 12,900 yr at Swiftcurrent Lake, Glacier National Park, Montana, USA

Kelly R. MacGregor [a,*], Catherine A. Riihimaki [b], Amy Myrbo [c], Mark D. Shapley [d], Krista Jankowski [a]

[a] Geology Department, Macalester College, St. Paul, MN 55105, USA
[b] Biology Department, Drew University, Madison, NJ 07940, USA
[c] LacCore, University of Minnesota, Minneapolis, MN 55455, USA
[d] Department of Geosciences, Idaho State University, Pocatello, ID 83209, USA

ARTICLE INFO

Article history:
Received 27 February 2009
Available online 19 September 2010

Keywords:
Glacier National Park
Radiocarbon dating
Lake sediment core
Holocene
Younger Dryas
Grain size
Total organic carbon
Mazama ash
Sunspot cycle
Solar forcing

ABSTRACT

Glaciated alpine landscapes are sensitive to changes in climate. Shifts in temperature and precipitation can cause significant changes to glacier size and terminus position, the production and delivery of organic mass, and in the hydrologic energy related to the transport of water and sediment through proglacial environments. A sediment core representing a 12,900-yr record collected from Swiftcurrent Lake, located on the eastern side of Glacier National Park, Montana, was analyzed to assess variability in Holocene and latest Pleistocene environment. The spectral signature of total organic carbon content (%TOC) since ~7.6 ka matches that of solar forcing over 70–500 yr timescales. Periodic inputs of dolomite to the lake reflect an increased footprint of Grinnell Glacier, and occur during periods when sediment sinks are reduced, glacial erosion is increased, and hydrologic energy is increased. Grain size, carbon/nitrogen (C/N) ratios, and %TOC broadly define the termination of the Younger Dryas chronozone at Swiftcurrent Lake, as well as major Holocene climate transitions. Variability in core parameters is linked to other records of temperature and aridity in the northern Rocky Mountains over the late Pleistocene and Holocene.

Introduction

Understanding controls on past climate variability is key to assessing potential future environmental change. The influence of solar forcing on climate during the Holocene has been increasingly documented in climate records (Lean and Rind, 1998); variability in solar strength has been tied to changes in North Atlantic climate through drift-ice proxies (e.g., Bond et al., 2001), changes in aridity/wetness inferred from microfossils (e.g., Magny et al, 2008; Plunkett and Swindles, 2008), changes in seasonal sedimentation resulting from monsoon shifts (e.g., Xiao et al., 2002; Xiao et al., 2006) and variability in the thickness of carbonate deposition due to temperature changes (e.g., Brauer et al., 2008). Oxygen isotope ratios, gypsum and biogenic silica abundance, and Mg/Ca ratios have also been used to demonstrate the role of solar irradiance in driving drought cycles or temperature variability (e.g., Yu and Ito, 1999; Hodell et al., 2001; Hu et al., 2003).

The climate history in the northern U.S. Rocky Mountains is known primarily from lacustrine paleoecological records that are widely spaced in Montana, Idaho, and Wyoming (e.g., Karsian, 1995; Doerner and Carrara, 1999; Millspaugh et al., 2000; Doerner and Carrara, 2001; Brunelle and Whitlock, 2003; Hofmann et al., 2006; Shapley et al., 2009; Shuman et al., 2009; Marlon et al., 2009). Modeling of western U.S. climate provides additional information about late Pleistocene and Holocene changes (e.g., COHMAP Members, 1988; Bartlein et al., 1998; Diffenbaugh et al., 2006). While several alpine lacustrine records span the Holocene in the Canadian Rocky Mountains (Reasoner et al., 1994; Reasoner and Huber, 1999; Leonard and Reasoner, 1999; Beierle et al., 2003), our knowledge of the timing of major climate shifts at high elevations in the northern U.S. Rocky Mountains is incomplete. Here we examine a ~12,900-year-long core from Swiftcurrent Lake and explore the relationship between climate forcing, glaciologic and geomorphic response to that forcing, and the resulting development and transport of clastic and organic material.

Field Setting

Swiftcurrent Lake (1490 m elevation) is located east of the Continental Divide in Glacier National Park, Montana, USA (Fig. 1). The northeastern basin of Swiftcurrent Lake has a catchment area of 44 km^2, and is fed by Swiftcurrent Creek and its tributaries. The southwestern basin of the lake has a catchment area of 36 km^2 that

* Corresponding author. Fax: +1 651 696 6122.
E-mail address: macgregor@macalester.edu (K.R. MacGregor).

0033-5894/$ – see front matter © 2010 University of Washington. Published by Elsevier Inc. All rights reserved.
doi:10.1016/j.yqres.2010.08.005

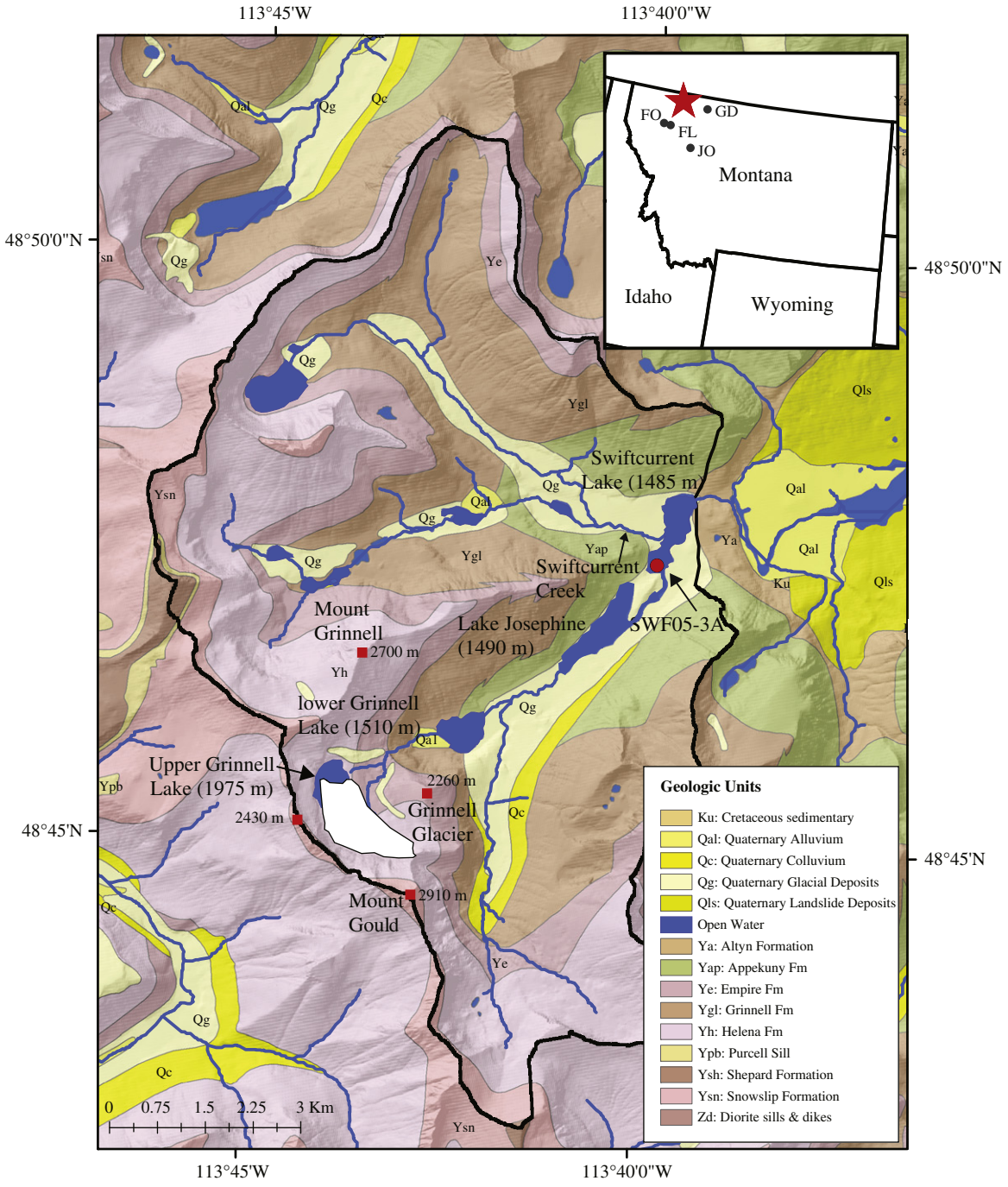

Figure 1. Map of the Many Glacier region of Glacier National Park, including Grinnell Glacier, Upper and Lower Grinnell Lakes, Josephine Lake, and Swiftcurrent Lake. Geologic units from Whipple, 1992. Location of Swiftcurrent Lake core SWF05-3A (white circle). Swiftcurrent Lake sits at 1486 m elevation, is 1.6 km long and ~0.5 km wide, narrowing to ~0.2 km at one point to form two lake subbasins, each between 5 and 10 m deep. Preliminary water depth measurements suggest the lake is roughly divided into a southwestern and northeastern subbasin. The subbasins are divided by a discontinuous ridge (water depths ~2–4 m) at the narrowest portion of the lake, which coincides with a topographic drainage divide. Water flows from southwest to northeast through the lake. There is an elevation change of 360 m between Upper and Lower Grinnell lakes, but just 20 m elevation change between Lower Grinnell and Swiftcurrent lakes. The lake bathymetry and surficial hydrology suggest that the coring site receives little if any sediment from Swiftcurrent Creek. Inset: Location of Glacier National Park, Montana (star). Other lake core locations in Montana referred to in the text are shown: JO = Jones Lake (Shapley et al., 2009), FL = Flathead Lake (Hofmann et al., 2006), FO = Foy Lake (Stevens et al., 2006; Stone and Fritz, 2006), GD = Guardipee Lake (Barnosky, 1989).

includes Grinnell Glacier (~2000 m elevation), Upper and lower Grinnell lakes, and Lake Josephine. Swiftcurrent Lake is 1.6 km long and ~0.5 km wide. Previous bathymetric mapping suggest the lake is roughly split into a southwestern and northeastern subbasin (each 5–10 m deep) that are divided by a discontinuous ridge (water depths ~3–4 m) at the narrowest portion of the lake, which coincides with a topographic drainage divide (U.S. Fish and Wildlife Service, 1980). The 6.58-m-long core from Swiftcurrent lake (SWF05-3A; Fig. 1) was collected from the center of the southwestern subbasin in ~8-m water depth. The coring site was ~200 m from the surrounding shorelines and downvalley from any deltaic features produced by the low-gradient inlet stream draining Josephine Lake. Core material was not

https://doi.org/10.1016/j.yqres.2010.08.005 Published online by Cambridge University Press

varved, but trace laminations existed in some sections. No sand, gravel, or till units were encountered during coring, and the core bottom reflected the limit of our physical capabilities.

The lake bathymetry and surficial hydrology suggests that the coring site receives little if any sediment from Swiftcurrent Creek. Steep hillslopes characterize the Grinnell Glacier (southern) valley; between Mount Grinnell and lower Grinnell Lake (~2-km distance) there is a 1-km change in elevation. The rock headwall around Grinnell Glacier is ~500 tall, and a 460-m-tall step in the valley between Upper and lower Grinnell lakes. The relief on the valley floor is low, with ~10-m elevation change between lower Grinnell and Swiftcurrent lakes. Relief in the basin diminishes toward Swiftcurrent Lake where the valley widens. In addition to glacially produced sediment, hillslope processes may play a role in stochastic sediment delivery to the lakes.

Geology and glacial history

The Swiftcurrent Lake drainage basin is underlain by the Middle Proterozoic Belt Supergroup, which is comprised primarily of siltsones, shales, and sandstones (Fig. 1; Horodyski, 1983). Grinnell Glacier is currently eroding the stromatolitic Siyeh limestone of the Helena Formation. The Siyeh limestone consists of dolomitic limestone and calcitic argillite (Whipple, 1992), and is the only bedrock source of dolomite in the valley.

Lake Josephine and Swiftcurrent Lake are underlain entirely by late Pleistocene tills 1–3 m thick (Earhart et al., 1989; Carrara, 1990; Whipple, 1992). The presence of Glacier Peak G ash (~13.1 ka; Mehringer et al., 1984) overlying this till in several locations in the Park (Carrara, 1989, 1993) suggests the valley below Grinnell Glacier was deglaciated before 13 ka. A minimum age of 11.4 ^{14}C ka BP for deposition in Otokomi Lake, located 10 km south of and ~500 m higher than Swiftcurrent Lake, supports this interpretation of widespread deglaciation in the valley before 11 ka (MacLeod et al., 2006; Carrara, 1989; 1995).

Methods

Core SWF05-3A was collected in July 2005 using the Livingstone-type coring technique (Wright, 1967, 1991). The core was logged, split, photographed, described using smear slides (Rothwell, 1989; Kelts, 2003), and subsampled at 1-cm resolution. We conducted several analytic measurements, including x-ray diffraction (XRD), grain size, carbon coulometry, and C/N elemental analysis. In addition, we collected samples for ^{14}C dating and for ash fingerprinting.

For XRD analysis, prepared samples were run on a Panalytical X'Pert Pro MPD. Qualitative analysis was conducted at 2-cm spacing and more frequently where dolomite was detected. Quantitative analyses were performed every 4th cm of core using both the clay fraction approach and the normalized relative intensity ratio (RIR) method (Moore and Reynolds, 1997; Hiller, 2003. Quantitative uncertainties are low (1–2%) when minerals comprise 30–70% by volume of a sample (e.g., 50 ± 1%), and slightly higher (~7%) for very low (<15%) or very high (>85%) concentrations.

Samples for grain size analysis were prepared by oxidizing organic matter with H_2O_2 and dissolving diatoms with an NaOH solution. Grain size was measured using a Horiba LA-920 Grain Size Analyzer using a refractive index of 116a001i (e.g., Sperazza et al., 2004), which has a range of 0.2 μm–2 mm grain-size detection. Quantitative assessment of grain size was performed every 4th cm of core.

Carbon coulometric analysis (Engleman et al., 1985) was conducted using a UIC Model 5011 CO_2 Coulometer. Analysis of total carbon (TC) was conducted continuously at 1-cm spacing. Replicate analyses were performed on 65 samples, with an average analytical 1σ uncertainty of ± 0.07% C (3.8% of the TC reading). Analysis of total inorganic carbon (TIC) was conducted on 16 samples from the top of the core, and averaged 0.13 ± 0.12%. TIC was <0.45% in all samples measured, and therefore we assume %TC ≈ %TOC for all samples.

C/N ratios reflect in-lake production of sedimentary organic matter, as well as the type and origin of organic material, e.g., the relative contributions of aquatic vs. terrestrial material (Meyers, 1994; Meyers and Teranes, 2001). Samples were run on a CE Instruments Elemental Analyzer (EA 1112), and C and N were measured as mass percent. C/N analyses were limited to every ~25 cm except in the lowest 0.5 m of core.

Three samples were collected for ^{14}C analysis. Charcoal-rich layers were identified and sieved to separate out the >63-μm portion. Charcoal separates and one terrestrial macrofossil sample were refrigerated in acidified deionized water before being shipped to the LLNL-CAMS facility for dating.

Distinctive volcanic ash (tephra) units provide both correlative and direct numerical age constraints (e.g., Sarna-Wojcicki et al., 2000). A 48-cm-thick layer dominated by volcanic ash was identified ~4.5 m below the sediment-water interface (Fig. 2). Tephra fingerprinting using INAA on the glass fraction was conducted at Washington State University (Borchardt et al., 1972).

Solar Forcing and Spectral Analysis

Spectral analysis is frequently used to assess periodicity in lake core records (e.g., Stone and Fritz, 2006; Stevens et al., 2006; Patterson et al., 2004). Spectral density is a measure of strength, or power, in the frequency band and can be used to infer consistent variations within the record. We used multitaper spectral processing to determine the spectral signature of %TOC and a Holocene proxy for solar forcing, a dendrochronologically dated ^{14}C record of the number of sunspots each decade over the last 11.4 ka (Solanki et al., 2004, 2005). We used Singular Spectral Analysis (SSA) to remove the first Principal Component (PC) from the %TOC and sunspot records, which

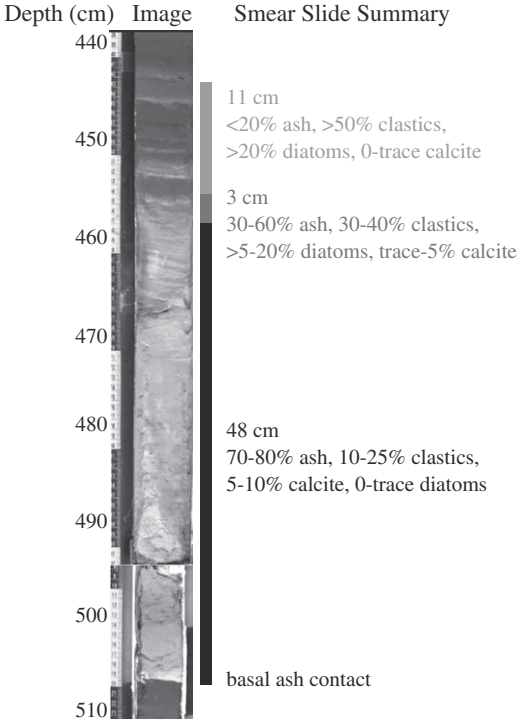

Figure 2. Image of Mazama ash in Swiftcurrent Lake core, including smear slide descriptions. Depth scale is distance below lake-sediment interface. Note the 48 cm of Mazama ash (black bar), a ~3-cm transition zone with 30–60% ash (dark gray), and ~4-cm-long zone with <20% ash (light gray). The majority of the ash layer was 70–80% ash (glass), 5–10% carbonate, and 10–20% clastic sediment. Diatoms were absent, or present only at the 1–2% level.

https://doi.org/10.1016/j.yqres.2010.08.005 Published online by Cambridge University Press

eliminates trends and long-period variations (Vautard and Ghil, 1989). We used an embedding dimension of 30 and eliminated PCs 13 through 30 because they were indistinguishable from white noise. These choices represent an even trade-off between resolution and confidence. We ran both Blackman–Tukey and Maximum Entropy spectral analyses using lags of 20% and 10%, respectively (Blackman and Tukey, 1958; Haykin, 1983).

Assessment of spectral strength is dependent on the assumption that the ages of the time series is well-known. Our age model for the period after 7.6 ka is better constrained than for the older portion of the record (see Age Model section), and we therefore conducted spectral analyses on the entire %TOC record, the most recent 7.6 ka, and on the period prior to 7.6 ka.

Results

Age model

Tephra analysis demonstrated a similarity coefficient of 0.98+ with the Mazama ash profile (Borchardt et al., 1972), with an age of 7630 ± 150 a (Zdanowicz et al., 1999). We quantified core composition across the Mazama ash unit (Fig. 2). The 48-cm-long ash layer was 70–80% ash (glass), 5–10% carbonate, and 10–20% clastic sediment. A 3-cm long transition zone comprised of 30–60% ash was present atop this unit, and ash percentages decreased to less than 30% within another 4 cm. We assume 48 cm of ash was deposited 'instantaneously' in time, and remove it from the age model (e.g., Beierle et al., 2003).

The age/depth relationship for SWF05-3A is shown in Figure 3a, and includes three calibrated radiocarbon ages (Table 1), the Mazama ash age of 7630 a, and an assumed age of −55 a (relative to AD 1950) for the top of the core. We use an age model with a linear fit between known ages, resulting in sedimentation rates ranging from 0.29 to 0.76 mm a^{-1} and an extrapolated age of 12.87 ka for the core-bottom (gray line, Fig. 3b). Although this model imposes step changes in the continuous sedimentation process, we feel that it is a reasonable reflection of our known ages and their associated uncertainties. The second-order polynomial age model (Fig. 3a, black line) falls near radiocarbon uncertainties, but we rejected this model as it overestimated by >400 yr the well-constrained Mazama ash age. We have high confidence in the age model between the Mazama ash and the core top because there are four age controls. The core below the Mazama ash represents ~5200 yr, based on the single ^{14}C age of 11.18 ± 80 cal yr BP. The time represented between the oldest radiocarbon date and the core bottom is 1690 yr.

Table 1
Results of radiocarbon analysis from LLNL CAMS and adjustment of ^{14}C age to calendrical age (CALIB 5.1).

LLNL/CAMSID number and material	^{14}C yr BP	1σ cal age range cal yr BP	2σ cal age range cal yr BP	Depth in core (m)	Median probability age (cal yr BP)
125098 charcoal	3160 ± 35	3358–3441	3273–3453	2.29	3388
124257 charcoal	3945 ± 35	4298–4506	4257–4517	3.065	4401
124258 charcoal	9760 ± 80	11093–11258	10788–11333	5.6	11180

$\delta^{13}C$ values were assumed to be −25‰ (Stuiver and Pollach, 1977) and the Libby half-life value of 5568 yr was used to calculate ages. Radiocarbon ages were converted to calendrical age using CALIB5.1.0 (after Stuiver and Reimer, 1993) using the Intcal04.14c calibration data set. Calibrated ages are shown as the full range of the 2-sigma age range calculated by CALIB.

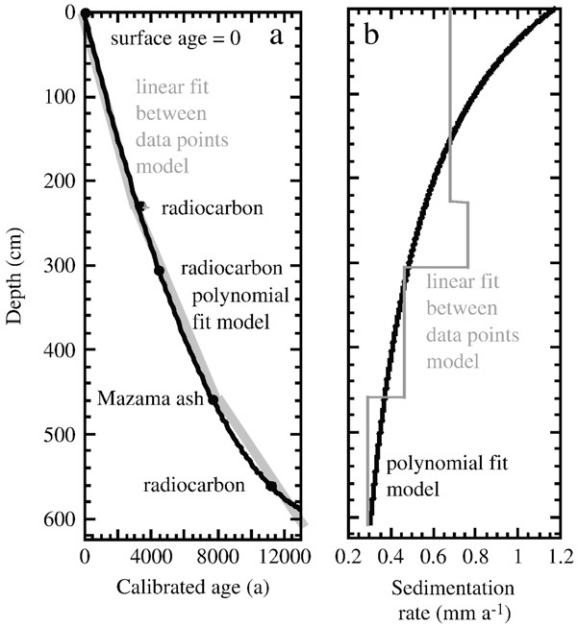

Figure 3. (a) Depth of three radiocarbon samples and Mazama ash in the Swiftcurrent Lake core. The black lines show the best-fit second-order polynomial model and the piecewise linear model of age (gray). The polynomial fit is well outside the Mazama ash age, with a model age >400 yr older than the known ash age. (b) Sedimentation rates assuming a polynomial age distribution of core sediment (black) and a piecewise linear fit (gray). Uncertainties in calendar ages are shown as age error bars; uncertainties are within the symbol size for most data.

Analytical results

Figure 4 shows major minerals, percent carbon and nitrogen, grain size, magnetic susceptibility, core density and sunspot number as a function of age, with the 48-cm Mazama ash layer removed. Major minerals (Fig. 4a) found throughout the core include quartz, illite, and chlorite; dolomite was identified at several locations in the core using both quantitative and qualitative measurements (Fig. 4b). With the exception of carbonates found in the Mazama ash layer, the dolomite grains have uneven margins and are rarely rhombohedral, suggesting they are detrital rather than authigenic. Illite comprises 6–13% of the inorganic material throughout the core. Quartz and illite percentages range between 35% and 55% and are anti-correlated.

Dolomite is present in fewer than 10% of >350 qualitative XRD samples. When present, dolomite is less than 2% by volume; this is equivalent to TIC of less than 0.26% in the sample, supporting our assumption that %TOC ≈ %TC.

TOC content varies from 0.75 to 5.25%, with most of the samples containing between 2 and 4% TOC (Fig. 4c). Nitrogen varies from 0.07 to 0.43%. The ratio of organic carbon to nitrogen (C/N) varies between 7.7 and 13 (Fig. 4d), typical of alpine lake sediment sourced primarily by algal material with some terrestrial carbon contribution (e.g., Fuji, 1988; Meyers and Horie, 1993).

Mean grain size varies from 2.5 to 20 μm, with an average of 7 μm for the core (Fig. 4e). Median grain size ranges from 1.5 to 13.2 μm. The peak in mean and median grain size at ~7.5 ka is associated with residual ash in the core, although five individual samples below the ash layer demonstrate increasing grain size beginning 8.25 ka. There are three distinct peaks in grain size between 3.8 and 1.3 ka.

Magnetic susceptibility (MS) in the core ranges from 5 to 20 × 10^{-6} SI (Fig. 4f). Core density increases abruptly from 1.2 to 1.4 g/cm^3 around 9.25 ka, and increases to 1.6 g/cm^3 toward the core bottom (Fig. 4 g).

https://doi.org/10.1016/j.yqres.2010.08.005 Published online by Cambridge University Press

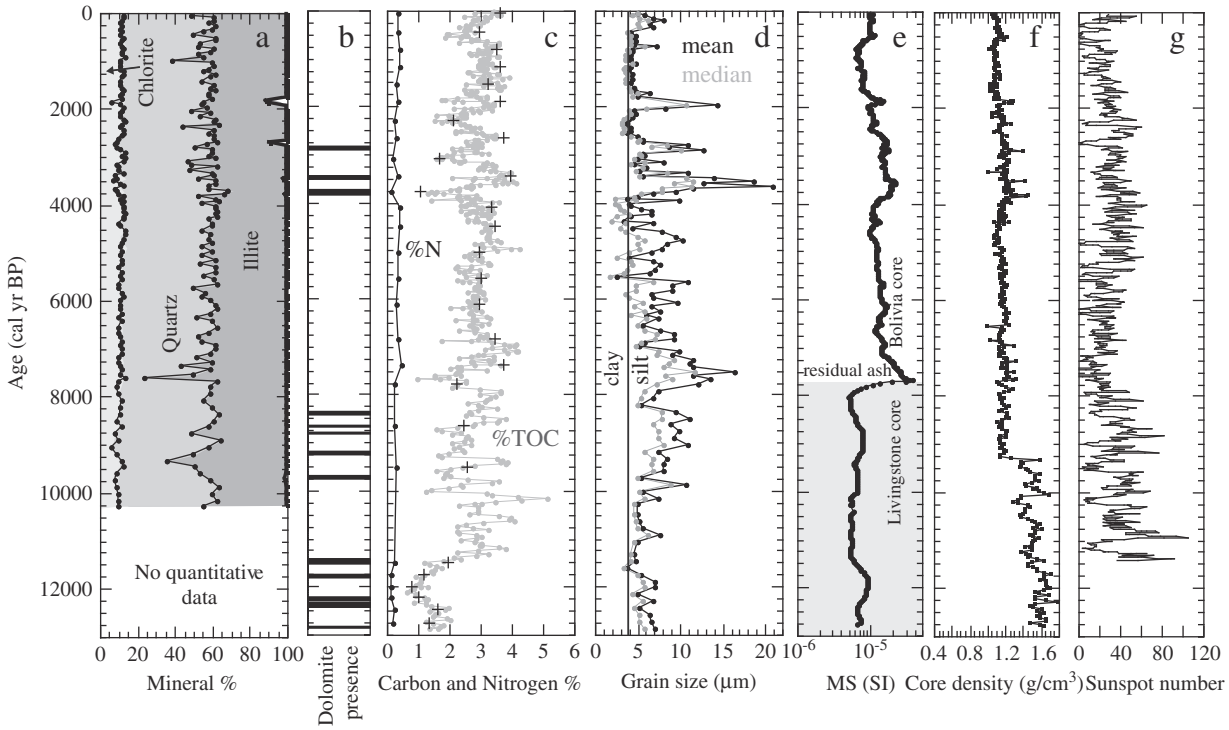

Figure 4. Swiftcurrent Lake core measurements over the past 12,900 yr. (a) Mineral percentages of chlorite, quartz, and illite are consistent throughout the core. The large illite spike at 7.6 ka corresponds with the top of the Mazama ash deposit. (b) Presence of dolomite (black bars), showing 1–2% dolomite in three "windows." Dolomite is present in three 'windows' in the core, between 2.8 and 3.8 ka, 8.3–9.75 ka, and from 11.4 to 12.8 ka. (c) Percent total organic carbon % (TOC; grey line), %TOC measured during C/N analysis (black crosses) and total nitrogen % (black line). (d) Mean (black) and median (gray) grain size. Mean and median values are typically silt sized (greater than 3.8 μm). (e) Magnetic susceptibility (SI units). The large spike in MS corresponds with the remnants of Mazama ash in the core, and the step change in density below results from a change in core diameter. (f) Core density increases with depth, from ~1.2 to 1.6 g/cm^3 (~25%). (g) Modeled sunspot number per decade from Solanki et al., 2004, 2005. High sunspot numbers correspond to increased solar output, or strength.

Spectral analysis

Blackman–Tukey spectral analysis of %TOC and solar strength (Fig. 4 g; Solanki (2005)) data from 7.6 ka to present show several major correlative and significant peaks (Fig. 5a). Much of the spectrum shows coherence at the 80%–90% level (Fig. 5b), with the greatest energy (strongest periodicities) at frequencies between 0.002 and 0.0145 a^{-1} (500–70 yr). We ignore coherence of the records at ages less than 70 yr because of substantially reduced spectral power in this range as well as the proximity to the Nyquist frequency. Figure 5c shows the results of the Maximum Entropy power spectrum, which tends to concentrate power in narrower bands compared to B–T analysis. Importantly, the Maximum Entropy shows coherent spectral power peaks at the same frequencies as the B–T analysis. The phase spectrum shows positive values at most of the coherent peaks, implying sunspots lead %TOC (Fig. 5c, inset). For most of the significant peaks in coherence with corresponding peaks in %TOC and sunspot energy, the phase lag is 30–50 yr. Our Nyquist frequency, based on the age model and sampling interval, is 0.02 yr^{-1}, or ~50 yr.

We note that the ~200-yr cycle is close to the 207-yr De Vries periodicity (Wagner et al., 2001). The spectral analyses show that the %TOC record has significant coherence with the sunspot record at the Gleissberg periodicity (~88 yr) (Yousef, 2006). There are parts of the power spectra where one record has a split peak so peaks do not correspond but there is still a significant coherence between the signals. For example, the %TOC peak at a frequency of 0.014 (~72 yr) corresponds at the 80% significance level with a split peak in the solar record between 0.0135 and 0.0145 (~68 and 76 yr). Spectral analyses performed across the entire 12.9 ka record showed diminished spectral energy and coherence; analyses performed on the record between 7.6 and 12.9 ka demonstrate insignificant coherence between the %TOC and sunspot records. It is not clear if this is because there is no statistically significant relationship between %TOC and solar strength from the latest Pleistocene to early Holocene, or if our single radiocarbon age control at 11.18 ka is insufficient to constrain the timing of variability in this period.

Discussion

Solar forcing of %TOC record

The striking correlation of the spectral power signature of %TOC and sunspot number (solar strength) leads to the hypothesis that organic carbon in Swiftcurrent Lake reflects solar output. The high degree of statistical certainty at well-known sunspot periodicities (Fig. 5) further supports this interpretation. While we did conduct spectral analyses over the entire period of record, the %TOC-solar irradiance relationship is clear only in the most recent 7600 yr. Notably, the general character of both the %TOC and sunspot record (Fig. 4a, g) between 7.6 and ~11.3 ka are marked by very large swings in %TOC over 50–250 yr timescales and are at odds with the rest of the records. External forces that could have an effect on the %TOC signal include variability in solar insolation (e.g., COHMAP Members, 1988; Berger and Loutre, 1991), remnants of the Laurentide Ice sheet influencing atmospheric circulation (e.g., Bartlein et al., 1998), and strong orographic gradients between lowland and alpine environments. Variability in sedimentation rates and %TOC could also be affected by post-glacial landscape stabilization in the early Holocene; coupled with the single radiocarbon date prior to 7.6 ka, is plausible that our age model is simply not sufficiently constrained in this window to show the %TOC/sunspot relationship.

https://doi.org/10.1016/j.yqres.2010.08.005 Published online by Cambridge University Press

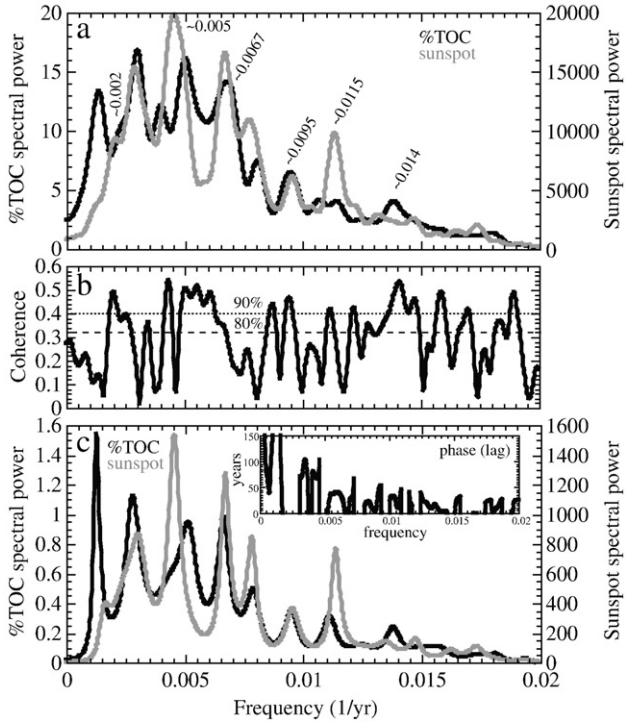

Figure 5. Spectral power of the %TOC (black line) and solar strength (gray line; Solanki, 2005) over the past 7600 yr. We used Singular Spectral Analysis (SSA) to remove the first Principal Component (PC) from the %TOC and sunspot records after truncating them at the Mazama ash. Removing the first PC eliminates trends and long-period variations. We used an embedding dimension of 30 and eliminated PCs 13 through 30 because they were indistinguishable from white noise. These choices represent an even trade-off between resolution and confidence. We ran both Blackman–Tukey and Maximum Entropy spectral analyses using lags of 20% and 10%, respectively. (a) Blackman–Tukey (B–T) power spectra as a function of frequency (yr^{-1}). *Y*-axis units are $\%^2$. (b) Coherence between the B–T power spectra of %TOC and solar strength. The 80% confidence interval is at 0.31 (dashed line), the 90% is at 0.4 (small dotted line). Approximately 10% coherence is expected in random (unrelated) records, with significantly more coherence observed in these records. (c) Using Maximum Entropy spectral analysis, the %TOC (black line) and solar strength (gray line) spectra show similar coherence to B–T between 0.002 and 0.014 (periods of ~70–500 yr). (c) inset, Phase spectrum (offset) between solar strength and %TOC. Positive values imply sunspots lead TOC. For most of the significant peaks in coherence with corresponding peaks in %TOC and sunspot energy, the phase is ~π/2, or a period of ~30–50 yr.

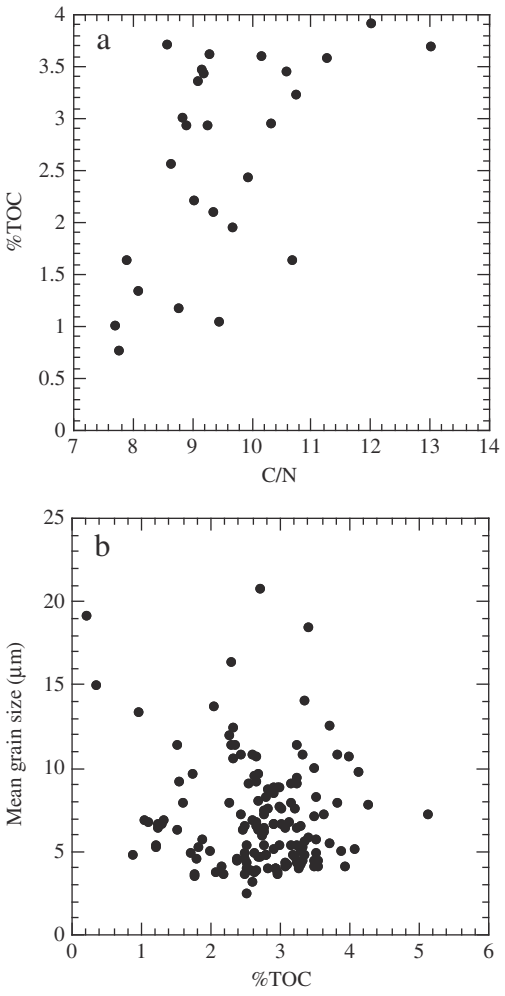

Figure 6. (a) Carbon/Nitrogen ratio vs. %TOC in Swiftcurrent Lake. The correlation suggests that our record reflects variable contributions of terrestrial organic matter in a lake that is sourced by lake algae (e.g., Meyers and Horie, 1993; Meyers and Lallier-Verges, 1999). (b) %TOC vs. mean grain size demonstrates there is no clear relationship between the amount of organic material and the grain size of clastic sediment.

Greater solar irradiance likely drives increased organic carbon deposition in Swiftcurrent Lake, with an average lag time of 30–50 yr (Fig. 5c, inset). The relationship between air temperature and greater total solar flux has been shown (e.g., Solanki et al., 2004). Several studies have shown a correlation between variability in solar output and biogenic silica levels, arguing that increased temperatures support higher diatom productivity (Hu et al., 2003; McKay et al., 2008). Wet periods have been linked to primarily algal sources of organic carbon (e.g., Meyers, 1993), although increased precipitation could also drive increased organic carbon transport into the lake. Asian monsoon cycles have also been linked to solar forcing and insolation (e.g., Clemens et al., 1991; Dykoski et al., 2005; Yuan et al., 2004) with monsoon intensity increasing with increased sunspot activity and/or number. While monsoon activity is obviously not expected here, there is evidence for significant lake-level changes (e.g., Shuman et al., 2009) and shifts in precipitation and aridity (e.g., Bartlein et al., 1998; Diffenbaugh et al., 2006; Marlon et al., 2009) throughout the late Pleistocene and Holocene.

An assessment of the source of the organic material based on C/N ratios can help clarify mechanisms of climate variability in the basin. There is a positive relationship between organic carbon and C/N ratios (Fig. 6a), which suggests that the C/N record reflects variable contributions of terrestrial organic matter rather than strictly changes in algal production rates (e.g., Meyers and Horie, 1993; Meyers and Lallier-Verges, 1999). The generally low C/N values in Swiftcurrent Lake are well-below the expected C/N value of terrestrial organic material (20 and greater), but the documented correlation between %TOC and C/N demonstrates that increased %TOC reflects increased terrestrial carbon inputs. Although selective diagenetic overprinting has been suggested as a potential cause of changes in C/N ratios (e.g., Spiker and Hatcher, 1984), our values of total organic carbon are quite low (1–5%) and therefore unlikely to be affected by diagenesis (e.g., Jasper and Hayes, 1990; Fontugne and Calvert, 1992). Our interpretation, based on a limited data set, is that higher C/N ratios reflect increased terrestrial inputs to the lake rather than increased lake productivity.

Percent TOC can vary as a result of changing glacigenic sediment flux into alpine lakes. Increased glacier size and/or proximity of a glacier terminus can lead to increased production and transport of glacially derived silt into a lake, thereby decreasing %TOC by dilution. Variability in organic carbon records has been used as a proxy for sediment flux in proximal glacial lakes (Karlen, 1976; Leonard, 1985, 1986, 1997). While Grinnell Glacier is upstream of Swiftcurrent Lake, surficial mapping of moraines in the Park suggest there have been at least two lake basins between Grinnell Glacier and Swiftcurrent Lake

https://doi.org/10.1016/j.yqres.2010.08.005 Published online by Cambridge University Press

since the end of the last glacial maximum (LGM: ~18 ka); we therefore expect a more complex the link between sediment flux and %TOC than in ice-proximal lake environments (e.g., Leonard and Reasoner, 1999). In addition, the C/N records suggest a variable but likely terrestrial source of organic material, which further implies that the %TOC record is not driven exclusively by inorganic sediment flux. There is no consistent relationship between grain size and %TOC for the entire period spanned by the core (Fig. 6b), although analysis of grain size at higher resolution is needed to draw conclusions from this result.

Dolomite presence and Grinnell Glacier

The presence of dolomite in Swiftcurrent Lake is a proxy for 'threshold' behavior of the drainage basin, in which glacial and hydrologic conditions are sufficient to move subglacially derived sediment downvalley to be deposited in the lake. We suggest that the dolomite signal reflects a combination of glacier size and hydrologic energy, in that both enhanced glacial erosion and increased peak summer water discharge are necessary to move dolomite to Swiftcurrent Lake. Dolomite presence may be more closely related to periods of glacial retreat, when the glacier footprint is large but when basal sliding, subglacial erosion, and water flux from ice melt are at a maximum (e.g., Koppes and Hallet, 2002). Given expected glacial erosion rates of ~1–10 mm yr^{-1} (e.g., Hallet et al., 1996; Riihimaki et al., 2005), the small amounts of dolomite found in Swiftcurrent Lake confirms there are spatial barriers to dolomite transport. Sediment must move through the proglacial hydrologic system and remain entrained through low-energy lakes to reach Swiftcurrent Lake. Because glacier size is a lagged response to both temperature and precipitation trends over seasonal to centennial timescales (e.g., Johannesson et al., 1989) dolomite presence should not be used as a temporally precise indicator of glacial maxima. If the contribution of dolomite from tills on the nearby hillslopes were significant, we might expect dolomite to have a presence throughout the core. We cannot rule out non-glacial stochastic hillslope delivery of dolomite to the lake (and in fact suggest this as one possible source of dolomite during the early Holocene), but argue that higher concentrations of dolomite might be expected from such events. Moreover, glacial erosion rates are typically an order of magnitude greater than fluvial or hillslope erosion rates (Hallet et al., 1996). The episodic transport of dolomite to Swiftcurrent Lake reflects variability in either the rate of subglacial erosion (which is tied to the amount of transportable dolomite produced), or the efficiency of transport of sediment through the lake systems.

With the links between organic carbon and solar strength, and between dolomite and glacial activity in mind, we discuss the core records within several discrete time periods (shaded bars, Fig. 7). We compare changes in our record to variability in North Atlantic temperatures as recorded in the GISP ice core (Fig. 7a; Alley, 2004). The GISP2 record offers a high-resolution hemispheric climatic context for our record of regional climatic and sediment-transport change.

Period I: ~12.9–11.3 ka

The %TOC record provides constraints on the termination of the Younger Dryas chronozone in the Glacier National Park region (Fig. 7a). The first 1000 yr are marked by very low %TOC values, and correspond with the coldest GISP2 temperatures between 12.9 ka and present (Fig. 7a). GISP2 temperatures increase rapidly between 11.8 and 11.5 ka, and then more slowly between 11.25 and 10 ka. Although

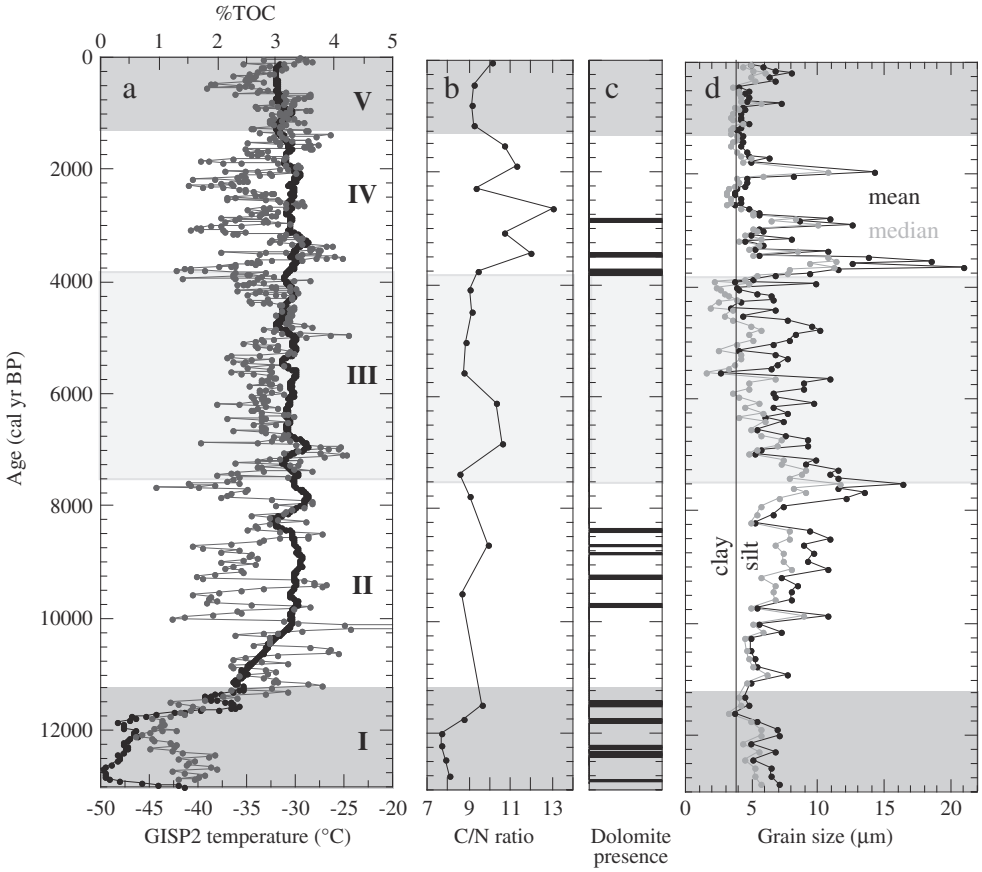

Figure 7. Core and hemispheric climate parameters over the past 12.9 ka. Periods I–V represent major transitions in the %TOC record from Swiftcurrent Lake. (a) GISP2 temperature (black line) and %TOC (dark gray). (b) C/N ratio, (c) Dolomite presence, (d) Mean (black line) and median (gray line) grain size.

https://doi.org/10.1016/j.yqres.2010.08.005 Published online by Cambridge University Press

the timing of variability in GISP2 and %TOC are not perfectly correlated, perhaps because of age uncertainty, %TOC values begin to increase rapidly at ~12 ka and are variable but generally higher after 11.5 ka. Typical termination dates for Younger Dryas (YD) chronozone are around 11.5 ka for the North Atlantic, when GISP2 temperatures transition from rapid to gradual warming. The Swiftcurrent %TOC record reflects an abrupt increase at ~11.5 ka that within dating uncertainties is synchronous with increasing GISP2 temperatures. This observation is consistent with lacustrine records from the Canadian Rocky Mountains ~400 km to the northwest that show Younger Dryas glacial advances occurring ~11.3 ^{14}C ka BP, with termination dates closer to 10.1 ^{14}C ka BP (Reasoner and Hickman, 1989; Reasoner et al., 1994; Reasoner and Huber, 1999; Beierle et al., 2003). Although the resolution is low, C/N values increase after ~12 ka and support abrupt change in the region during this time (Fig. 7b). Low C/N values prior to 12 ka suggest the organic carbon source is primarily (>50%) algal.

Mean and median grain size decreases between 12.9 and ~11.4 ka (Fig. 7d). A slight coarsening occurs between 11.4 and 10.8 ka. Decreased grain size of clastic sediments in lake cores could represent a shift to a deeper lake environment, but the Swiftcurrent outlet is bedrock-controlled and it is unlikely to have varied significantly over the Holocene. Several other western lakes are at lowstands during this period (Shuman et al., 2009), suggesting a more arid climate in the region. Coarser sediment is more likely to reflect geomorphic conditions in the watershed, with increased hillslope contributions to the lake, or increased the rate of surface water transport (glacial melt) through the chain of lakes in Swiftcurrent valley.

Our data suggest that between ~12.9 and 11.5 ka the Glacier National Park region was under a colder and possibly drier climate regime compared to the Holocene. The low %TOC and C/N values at the beginning of the period, and the subsequent rapid change in %TOC are coincident with warming in the GISP2 and Canadian Rocky Mountains lacustrine records. We interpret the %TOC, C/N and dolomite records as reflecting abrupt glaciological and sediment-transport changes consistent with warming from 11.3 to 11 ka.

Period II: 11.3 to ~7.5 ka (post-YD/early Holocene)

Percent TOC increases between 11.3 and 10 ka in concert with GISP2 temperatures, with the rest of Period II dominated by century-scale variations in TOC. There is a coarsening trend in Swiftcurrent Lake grain size, and dolomite is episodically present between 9.8 and ~8.3 ka.

Other studies in the northern Rocky Mountains suggest the early Holocene was a time of increased seasonality (e.g., Elias, 1996), with some areas of either extreme wet or dry summer months (Brunelle et al., 2005). The high variability in %TOC at Swiftcurrent Lake could reflect climatic extremes during Period II. Lacustrine records from the Rocky Mountains of Alberta suggest this period is one of severely limited ice extent, with restricted glacigenic sediment flux and arid conditions (Beierle et al., 2003; Reasoner and Huber, 1999). Proximal lowland cores show generally dry conditions during the early and mid Holocene (Whitlock, 1993; Shapley et al., 2009). If the dolomite is a response to increased glacier size, this is in contrast to other regional records that show extremely limited glacier extent (e.g., Carrara, 1987; Leonard and Reasoner, 1999). The presence of dolomite may reflect increased glacial hydrologic energy in Swiftcurrent basin (rather than increased glacier size), perhaps explained by a strong orographic effect and/or enhanced summer wetness (e.g., Bartlein et al., 1998; Shuman et al., 2009). It is notable that grain size is larger in the dolomite window, which might suggest a more proximal (hillslope) sediment source, perhaps a result of post-glacial landscape instability. While dolomite is not present in the core at the 8.2 ka cooling event (Morrill and Jacobsen, 2005), dolomite is found at 8.3 ka; our limited age controls may mask the evidence for this globally-recognized event. The Swiftcurrent record during Period II is complex, and likely reflects both variable climatic conditions as well as changing geomorphic conditions that are difficult to resolve entirely.

Period III: 7.5 to 3.8 ka (Middle Holocene)

The mid-Holocene at Swiftcurrent Lake is characterized by more stable and likely warmer environmental conditions compared to most of the Holocene, similar to observations in the Canadian Rocky Mountains (Reasoner et al., 1999; Beierle et al., 2003). 7–5 ka is a period of low %TOC variability, with a rapid rise and peak in %TOC from 7.5 to 7.0 ka, a peak in %TOC at 5 ka, and a rapid decrease at the termination of Period III (~4.2–3.8 ka). Dolomite is not present within this period; in concert with the generally high %TOC values we suggest Grinnell Glacier is likely smaller and/or less hydrologically vigorous than during Periods I-II. High, stable %TOC combined with a small or nonexistent Grinnell Glacier suggests climate was warmer overall during this time. The overall trend of decreasing grain size from the peak at 7.5 ka could be associated with decreased transport of sediment from hillslopes.

Aridity associated with the Holocene Thermal Maximum is observed in early Holocene in records from the northwestern U.S. (Barnosky et al., 1987; Thompson et al., 1993; Whitlock, 1993); in Guardipee Lake (Fig. 1, inset), pollen records indicate high early to mid-Holocene aridity relative to the present (Barnosky et al., 1987). In Jones Lake, MT, this period is marked by increasing moisture, in contrast to an early-Holocene (~9 ka) aridity maximum (Shapley et al., 2009). In pollen studies from the Colorado Rocky Mountains, Fall (1985) interpreted an increased altitudinal range of subalpine forests to represent a warmer and wetter climate between 7 and 4 ka. In contrast, Shuman and others (2009) show low regional water levels between 7 and 4.5 ka in the U.S. Rocky Mountains from Colorado to Montana. If we interpret the %TOC signal as reflecting temperature in the Swiftcurrent region, 7–4 ka is the warmest and most stable of the ~12,900-yr-long record.

Period IV: 3.8 to 1.3 ka (Late Holocene)

Major swings in climate conditions characterize the middle-late part of the Holocene at Swiftcurrent Lake, with large century- to millennial-scale variations present in the %TOC, grain size, and C/N records. The start of Period IV (Fig. 8) is well defined by a rapid coarsening of sediment, the presence of dolomite, and an increase in %TOC. Three notable %TOC excursions occur with minima at ~3.8, 3.05, and ~2.1–2.2 ka (dark gray bars, Fig. 8), and correlate with C/N decreases, although the resolution is low. The %TOC minima are associated with distinct coarsening events that lag them by ~50–150 yr (light gray bars, Fig. 8). It is notable that the peaks in C/N are higher during Period IV than during any other period. With the exception of the grain size peak at 7.5 ka (which incorporates residual silt-sized ash from the Mazama eruption), the three grain-size peaks during Period IV are higher than the rest of the record.

The concurrent variability in %TOC, C/N, and grain size, and the presence of dolomite, are strong evidence of variable climate affecting surface processes during this period. As %TOC and C/N rise, grain size in the core is generally high; as %TOC peaks at ~3.6, 2.6, and 1.6 ka, grain size is fine. This suggests that as climate transitions from cooler (low %TOC) to warmer (increased %TOC), there is coarse material coming off of hillslopes into the lake, perhaps as a result of diminished terrestrial vegetation on the landscape during cool periods. Increasing %TOC and C/N suggest concurrent warming and terrestrial carbon inputs; peaks in %TOC and C/N correspond to an overall decline in grain size, perhaps related to increased vegetative cover due to warmer conditions. Only the peak in grain size at 1.95 ka is correlative with a peak in %TOC; this is the only grain size peak in Period IV that is not related to glacial activity. We argue that increasing %TOC during

https://doi.org/10.1016/j.yqres.2010.08.005 Published online by Cambridge University Press

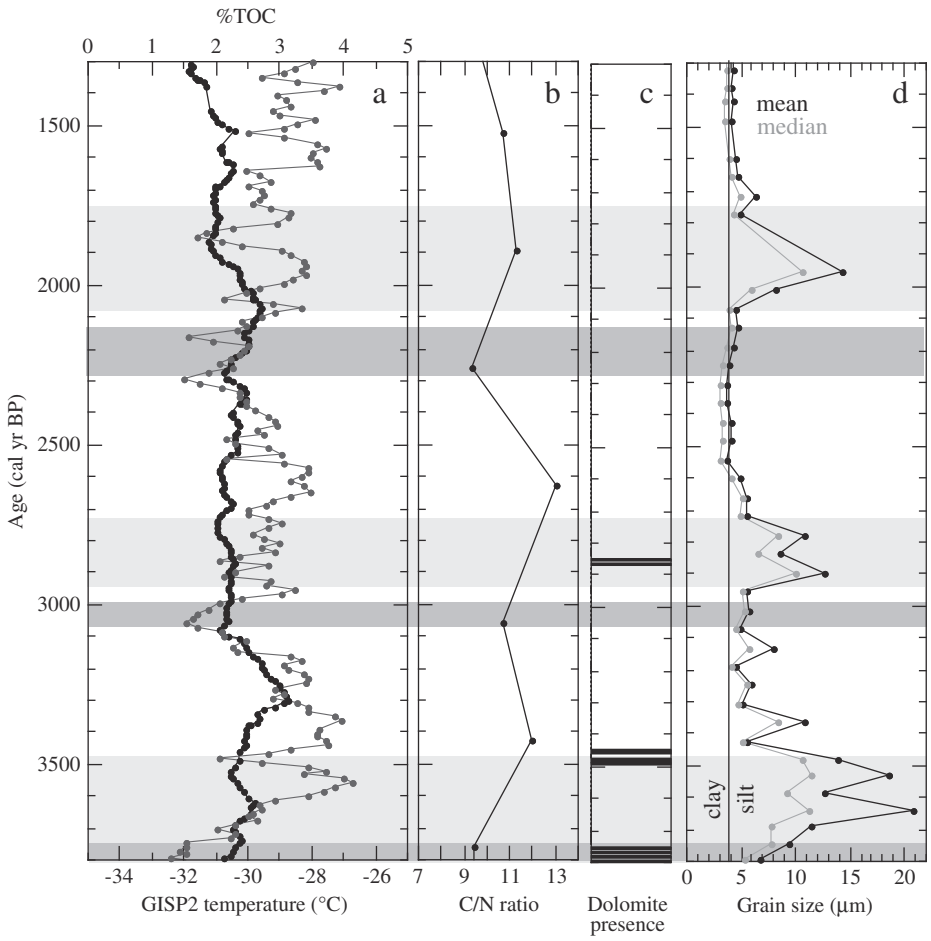

Figure 8. Period IV (3800–1300 cal yr BP) from Fig. 7, enlarged. (a) %TOC and GISP2 temperature, (b) C/N ratios, (c) dolomite presence, and (d) mean (black) and median (gray) grain size. Dark gray bars highlight zones of low %TOC, low C/N ratios, and fine-grained sediment, and light gray bars document subsequent grain size peaks. Increases in grain size lag %TOC minima by ~50–150 yr.

Period IV reflects increased temperatures and periods of terrestrial carbon dominance.

The presence of dolomite suggests enhanced glacial activity Grinnell Glacier between 3.8 and 2.8 ka. Dolomite presence corresponds with low %TOC and fine grain size at 3.75 and 3.5 ka, which we interpret as fine-grained glacial sediments in transport to Swiftcurrent Lake. The last evidence of dolomite in Period IV occurs at ~2.85 ka, and is associated with coarser grain sizes; this could reflect rapid glacier melting and retreat, transporting coarser particles to the distal lake as a result of increased erosion and hydrologic energy. There is supporting evidence for glacial advances in other parts of the northern Rocky Mountains during this period. High sedimentation rates in Hector Lake, Alberta, Canada between 3.5 and 2.9 ka suggest increased ice extent (Leonard, 1997) associated with the Peyto Advance (e.g., Luckman, 1993; Luckman, 1995). The presence of dolomite between 3.8 and 2.8 ka in Swiftcurrent Lake is correlative with this record, and we interpret the data as indicative of larger and/or more erosive Grinnell Glacier.

Evidence for climatic variability in the northern U.S. Rocky Mountains during this time shows a complex picture. Stone and Fritz (2006) argue that the region saw cyclic droughts alternating with less regular dry conditions after 4.5 ka. Data from Foy Lake suggest climate was dry and lake level was low between ~2.2 and 1.2 ka (Stevens et al., 2006), and Jones Lake trended episodically toward hydrologic freshening between 6 and 1.4 ka (Shapley et al., 2009). Several other lakes in Montana and Colorado show variable but generally increasing lake levels during this period (Shuman et al., 2009). Seismic reflection in Flathead Lake, MT, suggests a rise in lake levels between 7 and 1.6 ka, reflecting increasingly wet environments (Hofmann et al., 2006) culminating in a late-Holocene highstand contemporaneous with that of Jones Lake. The dry period identified in Foy Lake around ~2 ka is correlative with a coarse-grained sediment pulse and higher than average C/N ratios at Swiftcurrent Lake, indicating sediment and organic matter transport from the landscape. A dry period could explain the correspondence of high %TOC and C/N ratios with large grain size, and the absence of dolomite (lack of glacial advance/activity), in contrast to the earlier swings in the record during Period IV. Subsequent low %TOC and C/N ratios at ~1.8 ka suggest any dry period at Swiftcurrent Lake was short-lived.

Period V: 1.3 ka to present

The most recent period in the Swiftcurrent Lake core is characterized by generally high %TOC, low C/N ratios and fine-grained sediment (Fig. 7). Period V brackets well-defined climate events including the Medieval Warm Period (MWP) and the Little Ice Age (LIA), and changes in the %TOC record are well-correlated with documented timing of climate changes defining the MWP and LIA. For example, %TOC is relatively high and stable between 1.3 and 0.7 ka, corresponding closely with slightly increased GISP2 temperatures. The period from 1.1 to 0.8 ka was one of climatic quiescence at Foy Lake, MT (Stone and Fritz, 2006).

The initiation of the LIA is marked in the core by a sharp decline in %TOC at ~0.6 ka, and is followed ~200 yr later by a minor sediment

https://doi.org/10.1016/j.yqres.2010.08.005 Published online by Cambridge University Press

coarsening. Observations of Grinnell Glacier position show the glacier filled the cirque basin in 1850, and began its ongoing retreat thereafter (e.g., Carrara, 1987, 1993); this is consistent with known LIA glacier advances around the world. Interestingly, there is no dolomite measured in the core in the last ~2500 yr, which could mean the LIA advance was too short-lived to create or transport significant amounts of dolomitic sediment, or the glacial advance to the cirque margin was insufficient to increase dolomite flux. This is in notable contrast with interpretations of lacustrine records from the Canadian Rocky Mountains 400 km northwest of Swiftcurrent Lake that suggest the LIA glacial advance was the most extensive of the Holocene (e.g., Leonard and Reasoner, 1999).

Conclusions

A continuous core from Swiftcurrent Lake, Glacier National Park, MT spanning 12,900 yr demonstrates a strong link between climate in the basin and solar forcing on centennial timescales. The correlation between solar strength and %TOC confirms climate variability at Swiftcurrent Lake is related to solar forcing at 70–500 yr timescales during the past ~7.6 ka, with a lag of ~30–50 yr. Because %TOC variability is linked to solar forcing, it reasonably follows that the %TOC record from Swiftcurrent Lake provides constraints on climate conditions in the region. The interpretation of %TOC broadly reflecting temperature (i.e., low %TOC is associated with cold periods and high %TOC with warmer Holocene conditions) is broadly supported by paleoclimate studies in the region. While only a small portion of the drainage basin was glaciated during the past ~13 ka, we argue the record incorporates a "threshold" signature of glacial extent and hydrologic energy in the basin.

The use of Swiftcurrent Lake cores as a proxy for the hydrologic and geomorphic activity of Grinnell Glacier is complicated by the presence of three intermediate lake basins, and uncertainty associated with hillslope contributions to the lake. Quantifying the relationships between glacial erosion, hillslope failures, sediment transport and lake sedimentation will provide improved constraints on interpretations of climate proxies and alpine geomorphic processes.

Acknowledgments

We thank the Macalester College Wallace Faculty Research Fund (to KRM), the American Philosophical Society Lewis and Clark Research Fund (to CAR), and Dan Fagre, Blase Reardon, and the Many Glacier Park Rangers for financial and logistical support. Thanks to Kevin Thiessen for his generosity in the use of his Elemental Analyzer, and to Emily Dunn, Hannah Wydeven, Don Barber and Camille Jones for laboratory assistance. We thank the LacCore facility for field and lab support. Special thanks to Justin Revenaugh for assistance with the spectral analyses. We are grateful to Eric Leonard and an anonymous reviewer for helpful comments that improved the manuscript.

References

Alley, R.B., 2004. GISP2 Ice Core Temperature and Accumulation Data. Data Contribution Series #2004-013. NOAA/NGDC Paleoclimatology Program, Boulder, CO.
Barnosky, C.W., Grimm, E.C., Wright Jr, H.E., 1987. Towards a postglacial history of the Northern Great Plains: a review of the paleoecological problems. Annals of the Carnegie Museum 56, 259–273.
Bartlein, P.J., Anderson, K.H., Anderson, P.M., Edwards, M.E., Mock, C.J., Thompson, R.S., Webb, R.S., Webb III, T., Whitlock, C., 1998. Paleoclimate simulations for North America over the past 21, 000 years: Features of the simulated climate and comparisons with paleoenvironmental data. Quaternary Science Reviews 17, 549–585.
Beierle, B.D., Smith, D.G., Hills, L.V., 2003. Late Quaternary Glacial and environmental history of the Burstall Pass Area, Kananaskis Country, Alberta, Canada. Arctic, Antarctic, and Alpine Research 35 (3), 391–398.
Berger, A., Loutre, M.F., 1991. Insolation values for the climate of the last 10 million years. Quaternary Science Reviews 10, 297–317.
Blackman, R.B., Tukey, J.W., 1958. The Measurement of Power Spectra From the Point of View of Communication Engineering. Dover Publications, New York. 190 pp.
Bond, G., Kromer, B., Beer, J., Muscheler, R., Evans, M.N., Showers, W., Hoffmann, S., Lotti-Bond, R., Hajdas, I., Bonani, G., 2001. Persistent solar influence on North Atlantic climate during the Holocene. Science 294, 2130–2136.
Borchardt, G.A., Aruscavage, P.J., Millard Jr, H.T., 1972. Correlation of the Bishop Ash, a Pleistocene marker bed, using instrumental neutron activation analysis. Journal of Sedimentary Petrology 42, 301–306.
Brauer, A., Mangili, D., Moscariello, A., Witt, A., 2008. Palaeoclimatic implications from micro-facies data of a 5900 varve time series from the Pianico interglacial sediment record, Southern Alps. Palaeogeography, Palaeoclimatology, Palaeoecology 259, 121–135.
Brunelle, A., Whitlock, C., 2003. Postglacial fire, vegetation, and climate history in the Clearwater Range, northern Idaho, USA. Quaternary Research 60, 307–318.
Brunelle, A., Whitlock, C., Bartlein, P.J., Kipfmueller, K., 2005. Holocene fire and vegetation along environmental gradients in the northern Rocky Mountains. Quaternary Science Reviews 24, 2281–2300.
Carrara, P.E., 1987. Holocene and latest Pleistocene glacial chronology, Glacier National Park, Montana. Canadian Journal of Earth Sciences 24, 387–395.
Carrara, P.E., 1989. Late Quaternary and vegetative history of the Glacier National Park region, Montana.1902, 64
Carrara, P.E., 1990. Surficial geologic map of Glacier National Park. Montana 1 (100), 000.
Carrara, P.E., 1993. Glaciers and glaciation in Glacier National Park, Montana. Open-File Report 93–510, 1–18.
Carrara, P.E., 1995. A 12000 year radiocarbon date of deglaciation from the Continental Divide of northwestern Montana. Canadian Journal of Earth Sciences 32, 1303–1307.
Clemens, S., Prell, W.L., Murray, D., Shimmield, G.B., Weedon, G.P., 1991. Forcing mechanisms of the Indian Ocean monsoon. Nature 353, 720–725.
COHMAP Members, 1988. Climate changes of the last 18, 000 years: observations and model simulations. Science 271, 1043–1052.
Diffenbaugh, N.S., Ashfaq, M., Shuman, B., Williams, J.W., Bartlein, P.J., 2006. Summer aridity in the United States: response to mid-Holocene changes in insolation, ocean mean-state, and ocean variability. Geophysical Research Letters 33, L22712. doi:10.1029/2006GL028012.
Doerner, J.P., Carrara, P.E., 1999. Deglaciation and postglacial vegetation history of the West Mountains, west-central Idaho, U.S.A. Arctic, Antarctic, and Alpine Research 31, 303–311.
Doerner, J.P., Carrara, P.E., 2001. Late quaternary vegetation and climatic history of the Long Valley area, west-central Idaho, U.S.A. Quaternary Research 56, 103–111.
Dykoski, C.A., Edwards, R.L., Cheng, H., Yuan, D., Cai, Y., Zhang, M., Lin, Y., Qing, J., An, Z., Revenaugh, J., 2005. A high-resolution, absolute-dated Holocene and deglacial Asian monsoon record from Dongge Cave, China. Earth and Planetary Science Letters 233, 71–86.
Earhart, R.L., Raup, O.B., Whipple, J.W., Isom, A.L., Davis, G.A., 1989. Geologic maps, cross section, and photographs of the central part of Glacier National Park, Montana. .
Elias, S.A., 1996. Late Pleistocene and Holocene seasonal temperatures reconstructed from fossil beetle assemblages in the Rocky Mountains. Quaternary Research 46, 311–318.
Engleman, E.E., Jackson, L.L., Norton, D.R., 1985. Determination of carbonate carbon in geological materials by coulometric titration. Chemical Geology 53, 125–128.
Fall, P.L., 1985. Holocene dynamics of the subalpine forest in central Colorado; Late Quaternary vegetation and climates of the American Southwest. Contributions Series—American Association of Stratigraphic Palynologists 16, 31–46.
Fontugne, M.R., Calvert, S.E., 1992. Late Pleistocene variability of the carbon isotopic composition of organic matter in the Eastern Mediterranean; monitor of changes in carbon sources and atmospheric CO_2 concentrations. Paleoceanography 7, 1–20.
Fuji, N., 1988. Palaeovegetation and palaeoclimate changes around Lake Biwa, Japan during the last ca. 3 million years. Quaternary Science Reviews 7, 21–28.
Hallet, B., Hunter, L., Bogen, J., 1996. Rates of erosion and sediment evacuation by glaciers; a review of field data and their implications. Global and Planetary Change 12, 213–235.
Haykin, S., 1983. Nonlinear Methods of Spectral Analysis, 2nd ed. Springer-Verlag, Berlin.
Hiller, S., 2003. Quantitative analysis of clay and other minerals in sandstones by x-ray powder diffraction (XRPD). In: Worden, R.H., Morad, S. (Eds.), Clay Mineral Cements in Sandstones: Special Publication 34 of the International Association of Sedimentologists, pp. 213–251.
Hodell, D., Brenner, M., Curtis, J.H., Guilderson, T., 2001. Solar Forcing of Drought Frequency in the Maya Lowlands. Science 292 (5520), 1367.
Hofmann, M.H., Hendrix, M.S., Moore, J.N., Sperazza, M., 2006. Late Pleistocene and Holocene depositional history of sediments in Flathead Lake, Montana; evidence from high-resolution seismic reflection interpretation. Sedimentary Geology 184, 111–131.
Horodyski, R.J., 1983. Sedimentary geology and stromatolites of the Mesoproterozoic belt Supergroup, Glacier National Park. Precambrian Research, Montana. 20.
Hu, F.S., Kaufman, D., Yoneji, S., Nelson, D., Shemesh, A., Huang, Y., Tian, J., Bond, G., Clegg, B., Brown, T., 2003. Cyclic variation and solar forcing of Holocene climate in the Alaskan subarctic. Science 301, 1890–1893.
Jasper, J.P., Hayes, J.M., 1990. A carbon isotope record of CO_2 levels during the late Quaternary. Nature 347, 462–464.
Johannesson, T., Raymond, C.F., Waddington, E.D., 1989. A simple method for determining the response time of glaciers. In: Oerlemans, J., Bentley, C.R. (Eds.), Glacier fluctuations and climatic change. Oerlemans. Kluwer Academic Publishing.
Karlen, W., 1976. Lacustrine sediment and tree-limit variations as evidence of Holocene climatic fluctuations in Lappland, northern Sweden. Geografiska Annaler 58A, 1–34.

Karsian, A.E., 1995. A 6800-year vegetation and fire history in the Bitterroot Mountain Range, Montana. MSc. Thesis, University of Montana, Missoula. 54 p.
Kelts, K.R., 2003. Components in lake sediments: Smear slide identifications. In: Valero-Garcés, B.L. (Ed.), Limnogeology in Spain: A tribute to Kerry Kelts, pp. 59–72.
Koppes, M.N., Hallet, B., 2002. Influence of rapid glacial retreat on the rate of erosion by tidewater glaciers. Geology 30, 47–50.
Lean, J., Rind, D., 1998. Climate forcing by changing solar radiation. Journal of Climate 11, 3069–3094.
Leonard, E.M., 1985. Glaciological and climatic controls on lake sedimentation, Canadian Rocky Mountains. Zeitschrift Für Gletscherkunde Und Glazialgeologie 21, 35–42.
Leonard, E.M., 1986. Varve studies at Hector Lake, Alberta, Canada, and the relationship between glacial activity and sedimentation. Quaternary Rese 25, 199–214.
Leonard, E.M., 1997. The relationship between glacial activity and sediment production; evidence from a 4450-year varve record of Neoglacial sedimentation in Hector Lake, Alberta, Canada. Journal of Paleolimnology 17, 319–330.
Leonard, E.M., Reasoner, M.A., 1999. A continuous Holocene glacial record inferred from proglacial lake sediments in Banff National Park, Alberta, Canada. Quaternary Research 51, 1–13.
Luckman, B.H., 1993. Glacier fluctuation and tree-ring records for the last millennium in the Canadian Rockies; Decadal to millennial-scale variability in the climate system. Quaternary Science Reviews 12, 441–450.
Luckman, B.H., 1995. Calendar-dated, early "Little Ice Age" glacier advance at Robson Glacier, British Columbia, Canada. Holocene 5, 149–159.
MacLeod, D.M., Osborn, G., Spooner, J., 2006. A record of post-glacial moraine deposition and tephra stratigraphy from Otokomi Lake, Rose Basin, Glacier National Park, Montana. Canadian Journal of Earth Sciences 43, 447–460.
Magny, M., Gauthier, E., Vanniere, B., Peyron, O., 2008. Palaeohydrological changes and human-impact history over the last millennium recorded at Lake Joux in the Jura Mountains, Switzerland. The Holocene 18, 255–265.
Marlon, J.R., Bartlein, P.J., Walsh, M.K., Harrison, S.P., Brown, K.J., Edwards, M.E., Higuera, P.E., Power, M.J., Anderson, R.S., Briles, C., Brunelle, A., Carcaillet, C., Daniels, M., Hu, F.S., Lavoie, M., Long, C., Minckley, T., Richard, P.J.H., Scott, A.C., Shafer, D.S., Tinner, W., Umbanhowar Jr., C.E., Whitlock, C., 2009. Wildfire responses to abrupt climate change in North America. Proceedings of the National Academy of Sciences 106 (8), 2519–2524.
McKay, N.P., Kaufman, D.S., Michelutti, N., 2008. Biogenic silica concentration as a high-resolution, quantitative temperature proxy at Hallet Lake, south-central Alaska. Geophysical Research Letters 35 @Citation L05709.
Mehringer Jr, P.J., Sheppard, J.C., Foit Jr., F.F., 1984. The age of Glacier Peak tephra in west-central Montana. Quaternary Research 21, 36–41.
Meyers, P.A., 1994. Preservation of elemental and isotopic source identification of sedimentary organic matter. Chemical Geology 114, 289–302.
Meyers, P.A., Horie, S., 1993. An organic carbon isotopic record of glacial-postglacial change in atmospheric pCO_2 in the sediments of Lake Biwa, Japan. Palaeogeography, Palaeoclimatology, Palaeoecology 105, 171–178.
Meyers, P.A., Lallier-Verges, E., 1999. Lacustrine sedimentary organic matter records of late Quaternary paleoclimates. Journal of Paleolimnology 21, 345–372.
Meyers, P.A., Teranes, J.L., 2001. Sediment organic matter. In: Last, W.M., Smol, J.P. (Eds.), Tracking Environmental Change using Lake Sediments. Kluwer Academic Publishers, Drodrecht, pp. 239–269.
Millspaugh, S.H., Whitlock, C., Bartlein, P.J., 2000. Variations in fire frequency and climate over the past 17 000 yr in central Yellowstone National Park. Geology 28, 211–214.
Moore, D.M., Reynolds Jr., R.C., 1997. X-Ray Diffraction and the Identification and Analysis of Clay Minerals2nd ed. Oxford University Press, New York. 378 p.
Patterson, T.R., Prokoph, A., Chang, A., 2004. Late Holocene sedimentary response to solar and cosmic ray activity influenced climate variability in the NE Pacific. Sedimentary Geology 172, 67–84.
Plunkett, G., Swindles, G.T., 2008. Determining the sun's influence on late Glacial and Holocene climates: A focus on climate response to centennial-scale solar forcing at 2800 cal. BP. Quaternary Science Reviews 27, 175–184.
Reasoner, M.A., Huber, U.M., 1999. Postglacial palaeoenvironments of the upper Bow Valley, Banff National Park, Alberta, Canada. Quaternary Science Reviews 18, 475–492.
Reasoner, M.A., Osborn, G., Rutter, N.W., 1994. Age of the Crowfoot advance in the Canadian Rocky Mountains: A glacial event coeval with the Younger Dryas oscillation. Geology 22, 439–442.
Riihimaki, C.A., MacGregor, K.R., Anderson, R.S., Anderson, S.P., Loso, M.G., 2005. Sediment evacuation and glacial erosion rates at a small alpine glacier. Journal of Geophysical Research 110, F3. doi:10.1029/2004JF000189.
Rothwell, R.G., 1989. Minerals and mineraloids in marine sediments; an optical identification guide. Elsevier Appl. Sci, London, United Kingdom.
Sarna-Wojcicki, A.M., Lanphere, M.A., Champion, D.E., Clynne, M.A., Muffler, L.J.P., 2000. Revised age of the Rockland tephra, northern California; implications for climate and stratigraphic reconstructions in the western United States; discussion and reply. Geology 28, 286–287.
Shapley, M.D., Ito, E., Donovan, J.J., 2009. Late glacial and Holocene hydroclimate inferred from a groundwater flow-through lake, northern Rocky Mountains, USA. The Holocene 19 (4), 523–535.
Shuman, B., Henderson, A., Colman, S.M., Stone, J.R., Stevens, L.R., Fritz, S.C., Power, M.J., Whitlock, C., 2009. Holocene Lake-Level Trends in the Rocky Mountains, U.S.A. Quaternary Science Reviews 28, 1861–1879.
Solanki, S.K., Usoskin, I.G., Kromer, B., Schuessler, M., Beer, J., 2004. Unusual activity of the sun during recent decades compared to the previous 11, 000 years. Nature 431, 1084–1087.
Solanki, S.K., Usoskin, I.G., Kromer, B., Schuessler, M., Beer, J., 2005. 11,000 year sunspot number reconstruction. Data Contribution Series #2005-015, IGBP PAGES/World Data Center for Paleoclimatology. .
Sperazza, M., Moore, J.N., Hendrix, M.S., 2004. High-resolution particle size analysis of naturally occurring very fine-grained sediment through laser diffractometry. Journal of Sedimentary Research 74, 736–743.
Spiker, E.C., Hatcher, P.G., 1984. Carbon isotope fractionation of sapropelic organic matter during early diagenesis. Organic Geochemistry 5, 283–290.
Stevens, L.R., Stone, J.R., Campbell, J., Fritz, S.C., 2006. A 2200-yr record of hydrologic variability from Foy Lake, Montana, USA, inferred from diatom and geochemical data. Quaternary Research 65, 264–274.
Stone, J.R., Fritz, S.C., 2006. Multidecadal drought and Holocene climate instability in the Rocky Mountains. Geology 34, 409–412.
Stuiver, M., Pollach, H.A., 1977. Discussion: Reporting of ^{14}C data. Radiocarbon 19, 355–363.
Stuiver, M., Reimer, P.J., 1993. Extended ^{14}C database and revised CALIB radiocarbon calibration program. Radiocarbon 35, 215–230.
Thompson, R.S., Whitlock, C., Bartlein, P.J., Harrison, S.P., Spaulding, W.G., 1993. Climatic changes in the Western United States since 18, 000 yr B.P. In: Wright Jr, H.E., Kutzbach, J.E., Webb III, T., Ruddiman, W.F., Street-Perrott, Bartlein, P.J. (Eds.), Global climates since the last glacial maximum. University of Minnesota Press, Minneapolis, pp. 468–513.
U.S. Fish and Wildlife Service, 1980. Glacier National Park, fishery investigations, progress document, 1977, 1978, 1979, & 1980. Fish and Wildlife Center, Kalispell, MT.
Vautard, R., Ghil, M., 1989. Singular spectrum analysis in nonlinear dynamics, with applications to paleoclimatic time series. Physica D35, 295.
Wagner, G., Beer, J., Masarik, J., Muscheler, R., Kubik, P.W., Mende, W., Laj, C., Raisbeck, G.M., Yiou, F., 2001. Presence of the solar De Vries cycle (approximately 205 years) during the last ice age. Geophysical Research Letters 28, 303–306.
Whipple, J.W., 1992. Geologic map of Glacier National Parka, Montana.1:100,000..
Whitlock, C., 1993. Postglacial Vegetation and Climate of Grand Teton and Southern Yellowstone National Parks. Ecological Monographs 63 (2), 173–198.
Wright Jr, H.E., 1967. A square-rod piston sampler for lake sediments. Journal of Sedimentary Petrology 37, 975–976.
Wright Jr, H.E., 1991. Coring tips. Journal of Paleolimnology 6, 37–49.
Xiao, J., Nakamura, T., Lu, H., Zhang, G., 2002. Holocene climate changes over the desert/loess transition of north-central China. Earth and Planetary Science Letters 197, 11–18.
Xiao, S., Li, A., Liu, J.P., Chen, M., Xie, Q., Jiang, F., Li, T., Xiang, R., Chen, Z., 2006. Coherence between solar activity and the East Asian winter monsoon variability in the past 8000 years from Yangtze river-derived mud in the East China Sea. Palaeogeography, Palaeoclimatology, Palaeoecology 237, 293–304.
Yousef, S.M., 2006. 80-120 yr long-term solar induced effects on the earth, past and predictions; long term changes and trends in the atmosphere. Physics and Chemistry of the Earth 31, 113–122.
Yu, Z.C., Ito, E., 1999. Possible solar forcing of century-scale drought frequency in the northern Great Plains. Geology 27, 263–266.
Yuan, D., Cheng, H., Edwards, R.L., Dykoski, C.A., Kelly, M.J., Zhang, M., Qing, J., Lin, Y., Wang, Y., Wu, J., Dorale, J.A., An, Z., Cai, Y., 2004. Timing, duration, and transitions of the Last Interglacial Asian monsoon. Science 304, 575–578.
Zdanowicz, C.M., Zielinski, G.A., Germani, M.S., 1999. Mount Mazama eruption; calendrical age verified and atmospheric impact assessed. Geology 27, 621–624.